Electrochemical degradation of norfloxacin using BDD and new Sb-doped SnO$_2$ ceramic anodes in an electrochemical reactor in the presence and absence of a cation-exchange membrane

J. Mora-Gomez[1], E. Ortega[1], S. Mestre[2], V. Pérez-Herranz[1], M. García-Gabaldón[1*]

[1]IEC Group, ISIRYM, Universitat Politècnica de València, Camí de Vera s/n, 46022, València, P.O. Box 22012, E-46071, Spain
[2]Instituto Universitario de Tecnología Cerámica, Universitat Jaume I, Castellón, Spain.

*Corresponding author: mongarga@iqn.upv.es

Abstract

Electrochemical oxidation of Norfloxacin (NOR) in sodium sulphate media has been comparatively studied in an undivided and in a divided electrolytic cell both containing either a boron doped diamond (BDD) or a novel Sb-doped SnO$_2$ ceramic anode under galvanostatic operation. The electro-oxidation was found to occur with first order kinetics mainly when using both anodes. The results showed the great oxidizing power of BDD in relation to the ceramic anode to convert NOR and all the intermediate accumulated into CO$_2$. In the case of the BDD, although a 92 % of TOC abatement was achieved, the complete mineralization was not possible probably due to the carboxylic acids still present in solution. On the contrary, for the ceramic electrode, which presented a maximum value of TOC removal of about 63 %, the total mineralization of the aromatic oxidation intermediates was not reached under the experimental conditions.

 The use of a membrane divided cell showed positive aspects in terms of molecule degradation, degree of mineralization and current efficiency since prevents the intermediate products formed during the NOR oxidation process from being reduced on the cathode.

Keywords: BDD anode, SnO$_2$ ceramic anode, electrochemical oxidation, Norfloxacin, total organic carbon.

1. **Introduction**

In recent years, pharmaceuticals and personal care products have been identified as emerging contaminants threatening natural environment and human health, being the antibiotics one important category of these trace organic contaminants [1]. The presence of antibiotic compounds in surface waters is an emerging environmental issue since many of these substances are not biodegradable, toxic and capable of accumulating in single aquatic organisms (algae). Antibiotics might also lead to adverse environmental effects, including the development of antibiotic resistance to aquatic bacteria, direct toxicity to microorganism and possible risks to human health through drinking water and/or food-chain [2].

Pharmaceuticals industries, hospitals or simple civil buildings represent important points of antibiotic discharge into the environment, which produce a non-negligible effect on the physical, chemical and biological composition of receptor water bodies [3]. In fact, occurrence of antibiotics in the environment has been reported worldwide, such as in rivers of Europe [4,5] surface water of America [4,6], rivers of Australia [7] and seas and rivers of Asia [8,9].

Fluoroquinolones are a type of antibiotics applied in veterinary and human medicine since they were developed in the 1980s. Norfloxacin belongs to fluoroquinolone antibiotics, and has been used to treat a wide range of gastrointestinal, urinary and respiratory tract infections; ocular and skin infections as well as in patients with intraabdominal infections in combination with antianaerobic agents [10].

These compounds are not effectively removed from contaminated urban wastewaters by conventional municipal treatment plants [11] and may be transferred to soil treated with the digested sludge as fertilizer [12], thus representing an additional entry route into the environment. Several water treatment technologies have been investigated for the removal of organic load from contaminated effluents. Additional treatment techniques, such as membrane processes [13,14] or methods based on adsorption processes, such as biosorption onto microbial biomass [15], adsorption on carbon nano-tubes [16] or in magnetic molecular imprinted chitosan/y-Fe_2O_3 [17] has been investigated. However, they only transfer the contamination from one phase to another and the further disposal and treatment of adsorbents limit their application.

Therefore, powerful methods must be developed and applied to remove these pollutants from wastewaters for avoiding their possible adverse health effects on humans, animals and the environment. Several advanced oxidation processes may be used to remove antibiotics from wastewater, but ozonation, Fenton/photo-Fenton and photocatalysis have been the most tested ones [18,19]. Numerous researches have

promoted the electrochemical oxidation as a promising alternative technique to treat wastewaters containing toxic and/or refractory organic pollutants [3,19,20]. Versatility, efficiency, good cost-effective relationship, easy automatization, and environmental-friendly are among the main attractive characteristics of this technology [20].

Electro-oxidation of organic pollutants can be performed in several different ways, including direct oxidation, in which the pollutant is oxidized by electron transfer directly to the anode material; and indirect oxidation, in which the electron transfer is mediated by an oxidant species [21]. This depends on the interaction between the hydroxyl radical and the anode material. In this way, anodes with low oxygen evolution overpotential (low oxidation power anodes) like Pt, IrO_2 and RuO_2 yield chemisorbed "active oxygen" and only permit the partial oxidation of organics, while anodes with high oxygen evolution overpotential (high oxidation power anodes) like boron-doped diamond (BDD), PbO_2 and SnO_2, which have a "nonactive" behavior, yield physisorbed ·OH radicals and favor the complete oxidation of the organics to CO_2. In this context, BDD anodes have the highest overpotential for oxygen evolution and have been largely used in the electrochemical degradation of pollutants [21–23].

In this context, several investigations have been conducted on the removal of fluroquinolones by electrochemical oxidation. Coledam et al. [19] evaluated the electrochemical mineralization of NOR using a filter-press flow reactor with BDD anodes of distinct characteristics. The small number of aromatic by-products formed and the high values of the extent of electrochemical combustion attested the high oxidation power of the BDD anode, which led to a high CO_2 conversion independently of the boron-doping level. Jara et al. [3] performed electrooxidation tests in solutions containing two types of antibiotics with different electrodes. Among the different anodes tested, the Ti/Pt electrode showed the highest specific electrocatalytic activity towards organic oxidation due to the strong tendency of organic species to adsorb on the platinum electrode surface, as well as by its easy generation of active oxygen species. The DSA type electrodes have rather limited oxidative performances, mainly since they favor both a direct oxygen production from water electrolysis and worse adsorption characteristics of the organic molecules with respect to the Ti/Pt electrode. The electrochemical degradation of the fluoroquinolone antibiotic norfloxacin (NOR) on Ti/IrO_2 anodes, in several aqueous matrices was also evaluated by Sierra et al. [20]. The results revealed that the degradation of NOR could occur through both direct elimination at the electrode surface and mediated oxidation, via the electrogeneration of oxidative agents, such as active chlorine species and percarbonate ions.

Sb-doped SnO_2 electrodes have been also widely applied to treat different organic pollutants containing antibiotics due to numerous advantages, such as high oxygen

evolution over-potential, excellent electro-catalytic performance, cost efficiency and ease of preparation [24]. However, their major drawback is a low stability under anodic polarization that limits their practical applications [25].

A possible alternative are the Sb-doped SnO_2 ceramic electrodes. Massive ceramic electrodes are becoming important in the electrochemical technology such in fuel cells [26,27] and in electrochemical wastewater treatment [28–30]. These promising electrodes present a low price, a high active area due to its porosity; a high chemical stability and their manufacture is relatively easy [31]. Taking into account that the electrooxidation of fluoroquinolone antibiotic has been scarcely investigated, the aim of the present work is to compare the performance of a new microporous Sb-doped SnO_2 ceramic electrode with that of a BDD electrode. These electrodes have been applied to the electrochemical degradation of NOR in an electrochemical cell in the presence and absence of an ion-exchange membrane.

2. Experimental.

Solutions composed of 100 mg·L^{-1} of NOR (Sigma-Aldrich) and 2 g·L^{-1} of Na$_2$SO$_4$ as supporting electrolyte were treated in the undivided reactor which consists of a Pyrex glass of 250 cm^3 whereas the two-compartment electrochemical reactor containing the ionic membrane is made of two Pyrex glass chambers with a Nafion 117 (from Dupont) cation-exchange membrane placed between them. An equal volume (250 cm^3) of anolyte and catholyte was poured in their respective chamber after cell assembly. The same solution as that used in the undivided reactor was filled in the anodic compartment whilst in the cathodic compartment of the divided reactor, a solution composed of 2 g·L^{-1} of Na$_2$SO$_4$ was used as electrolyte. The solutions were vigorously stirred with a magnetic bar to ensure mixing and the transport of reactants. Na$_2$SO$_4$ was of analytical grade from Panreac. All solutions were prepared using distilled water.

In both cases, the electrode acting as counter electrode was a 20 cm^2 AISI 304 stainless steel sheet and a standard Ag/AgCl saturated KCl electrode was used as the reference electrode. Two different materials were tested as anode: a Boron-doped diamond (BDD) electrode with a doping level of 2500 ppm purchased from NeoCoat SA (Switzerland), and a new microporous Sb-doped SnO$_2$ ceramic electrode, both with a submerged geometric surface area of 12 cm^2.

The synthesis of the ceramic electrode is well described in a previous work [31]. A prismatic specimen of 80 x 20 x 5 mm was obtained by unidirectional dry pressing at 250 kg·cm^{-2} with a laboratory uniaxial manual press (Robima S.A., Spain). Finally, the sample was sintered in a laboratory furnace (RHF1600, Carbolite Furnaces, UK) at a temperature of 1200 ºC, heating at 5 ºC·min^{-1} from room temperature to the maximum temperature. It was kept one hour at the maximum temperature and then cooled. The electrical resistivity of the sintered sample was measured by a four points method with a Fluke 743B equipment (Fluke Corporation, USA), with a homemade setup. Then, bulk density was also measured by mercury immersion. The pore size distribution was obtained by mercury intrusion (AutoPore IV 9500, Micromeritics, USA). In addition, SEM images were taken with a FEG-SEM (QUANTA 200 F, FEI Co, USA) from polished sections of the sintered specimen.

Electrolysis experiments were performed under galvanostatic control at different applied current densities (33, 50 and 83 mA·cm^{-2}) using a power supply. Samples were taken from the electrochemical reactor every 30 min, and electrode potential, current and cell voltage, were recorded during the electrolysis. The degradation was followed by measuring the change in the absorbance at 275 nm using an Unicam UV4-200 UV/vis Spectrometer [32]. Mineralization of NOR was followed by total organic carbon

(TOC) determined on a Shimadzu TNM-L ROHS TOC analyzer. Measurement of inorganic ions (NH_4^+, NO_3^- and F^-) was performed on a Metrohm Ionic Chromatograph 883 Basic IC Plus. All the experiments were performed at room temperature during 4 hours.

From these data, the extent of the electrochemical combustion (ϕ) of the removed NOR [33] was calculated as the ratio between the percentages of [TOC] and [NOR] removal [19,33]:

$$\phi = \frac{\%TOC_{removed}}{\%NOR_{removed}} \tag{1}$$

ϕ is an indicative of the conversion rate of the NOR molecules into CO_2, therefore, this parameter presents values between 0, without combustion, or 1, with total combustion, in relation with the initial compound removed.

The mineralization current efficiency (MCE) values at a given time t (min) were computed according to the following equation [34,35]:

$$MCE = \frac{nFV\Delta(TOC)_t}{7.2 \times 10^5 \, mIt} \tag{2}$$

Here $\Delta(TOC)_t$ is the removed organic carbon (mg carbon·L^{-1}) at a given time, n is the number of electrons exchanged in mineralization process, m is the number of carbon atoms in a norfloxacin molecule (16), F is Faraday constant (96,487 C·mol^{-1}), V is volume of the treated solution (L), I is the applied current (A) and 7.2×10^5 is the conversion factor for homogenization of units (60 s·min^{-1} x 12,000 mg carbon·mol^{-1}). The number of electrons exchanged in the mineralization process per mole of NOR was assumed as 66 considering that the overall mineralization of the antibiotic involves its conversion into CO_2, F^- and mainly NH_4^+ from N degradation via reaction [36]:

$$C_{16}H_{18}FN_3O_3 + 29\,H_2O \longrightarrow 16CO_2 + 3NH_4^+ + F^- + 64H^+ + 66e^- \tag{3}$$
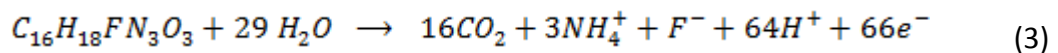
3. Results

Regarding with the ceramic electrode characterization, the measurement of the resistivity of the sample, gave a value of 0.0411 Ω·cm, which is low enough to be used as electrode. The pore size distribution of the sintered sample reveals a mean value of pore diameter of 0.24 μm (Figure 1) and an open porosity of 47.7 %. On the other hand, the SEM image of the ceramic electrode (inset of Figure 1) shows the pores distributed along the ceramic matrix as larger white particles.
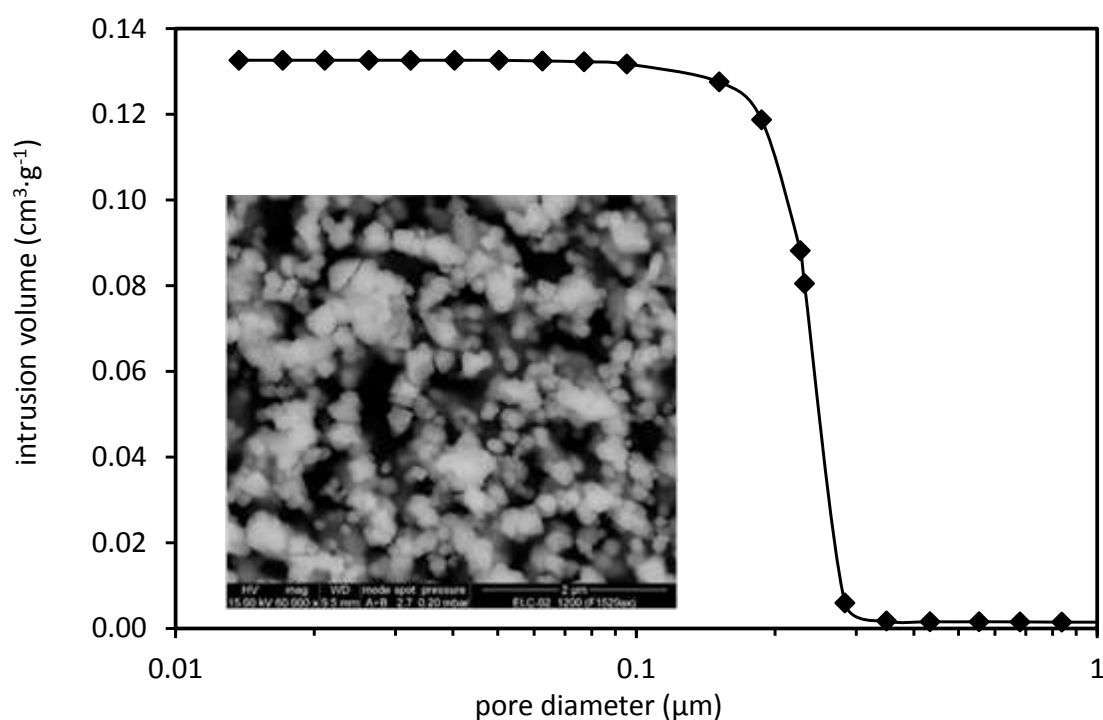

Figure 1. Pore size distribution of the ceramic electrode sintered at 1200 ºC. Inset: SEM image

The effect of the applied current density (i) on the kinetics of NOR degradation in the divided and undivided reactors using the BDD and the ceramic electrodes is studied in Figures 2 a) and 3 a), respectively. As shown in both figures, the higher the applied current the higher the velocity of the NOR degradation. For an electrolysis time of 30 minutes, in the case of the BDD electrode, the percentages of NOR degradation in the undivided reactor were 40%, 51% and 64% for the corresponding current densities of 33, 50 and 83 mA·cm^{-2}, and 64%, 81% and 92% for the same current densities in the case of the divided reactor. For the ceramic electrode, the percentages of NOR degradation were 15%, 30% and 46% in the undivided reactor, and 29%, 42% and 51% in the divided one.

The increase of the velocity of the NOR degradation with the applied current is mainly due the enhancement of the generation of active oxidant species, especially the ·OH radicals formed at the surface of the anode, which improve the destruction of the organic pollutants [37]. Hence, the BDD electrode allows a very weak electrode-·OH interaction which results in a much greater O_2-overvoltage than in the case of SnO_2 (ceramic electrode). This have been confirmed in the voltammograms obtained for BDD and the ceramic electrodes (not shown) which revealed that the Sb-SnO_2 ceramic electrode presents an onset potential of 1.9 V O_2 evolution, consistent with the literature data [38], whereas that obtained for the BDD was 2.5 V. All this data has been included in our previous work [31]. The much higher onset potential for O_2 evolution of the BDD explains why this electrode possesses is more efficient for pollutant oxidation.

Additionally, Figures 2 b) and 3 b) show the decay of the relative NOR concentration as a function of the applied charge per unit volume of electrolyzed solution (Q) in the divided and undivided reactors using the BDD and the ceramic electrodes, respectively. It is interesting to note that in each reactor, the curves are overlapped as the process is under mass transport control, and the electrooxidation process only depends on the transport of the organic species from the bulk solution to a region close to the anode [19].

For a given value of current density and for both electrodes under study, the velocity of NOR degradation is always higher in the presence of the cation-exchange membrane, since it allows to have an acid environment in the anodic compartment which enhances the kinetics of electron transfer and chemical reaction. Indeed, acid dissociation represents a precursor reaction for the electrochemical oxidation pathway [3]. In this sense, it must be highlighted that the complete NOR degradation is possible after 60 minutes of electrolysis using the BDD electrode in the electromembrane reactor for the applied currents densities of 50 and 83 mA·cm^{-2}.

Moreover, ions chromatograms obtained in the treated solutions at the end of the electrolysis revealed the accumulation of NH_4^+ and F^- in all cases for every reactor and electrode under study. Nitrate ions concentration was negligible in comparison to that of ammonium.
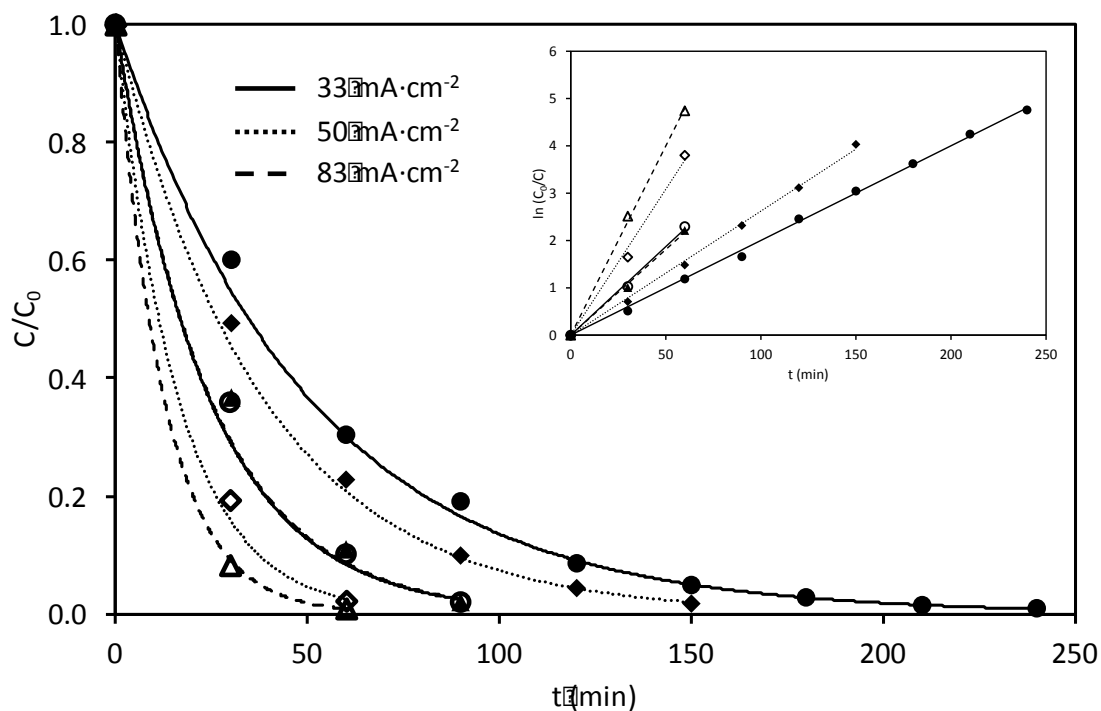
Figure 2 a). Effect of i on the decay of the relative concentration of NOR as a function of time for the BDD electrode. Solid points represent the reactor without membrane and empty points the membrane reactor.
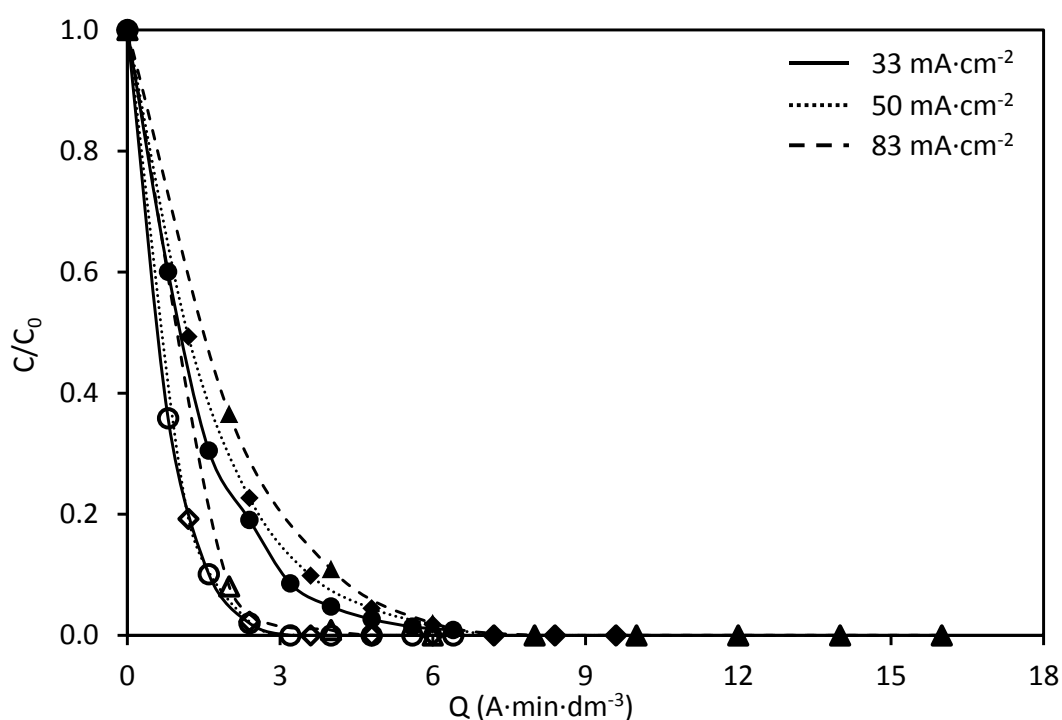

Figure 2 b). Effect of i on the decay of the relative concentration of NOR as a function of the applied charge per unit volume of electrolyzed solution for the BDD electrode. Solid points represent the reactor without membrane and empty points the membrane reactor.
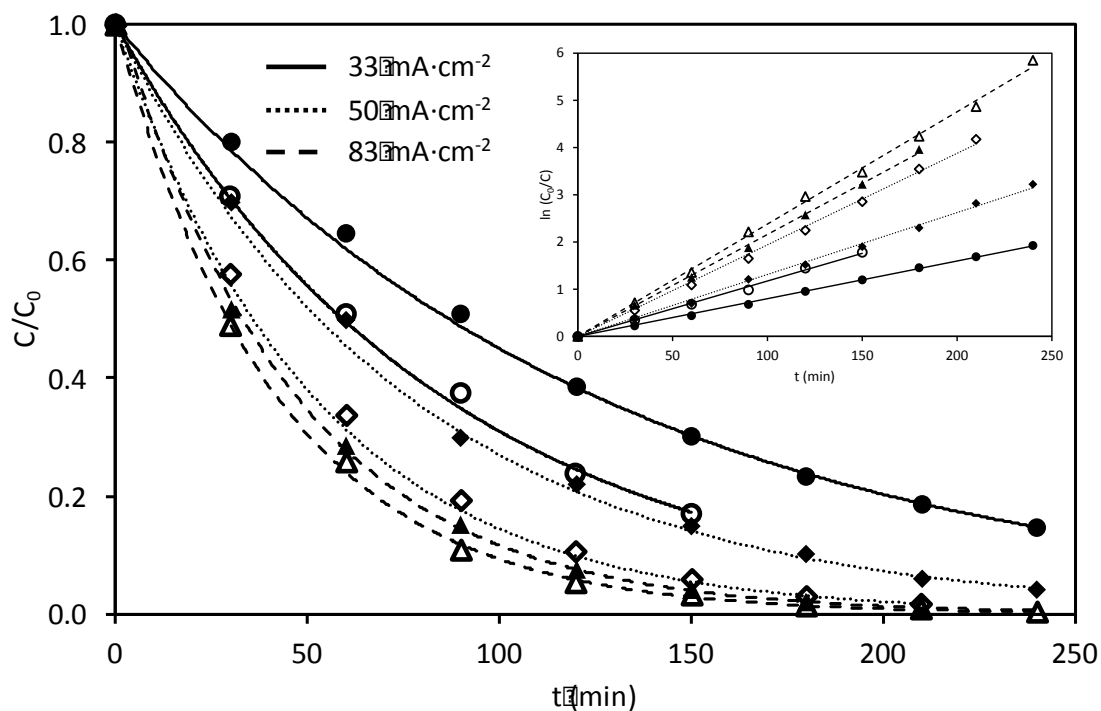
Figure 3 a). Effect of i on the decay of the relative concentration of NOR as a function of time for the ceramic electrode. Solid points represent the reactor without membrane and empty points the membrane reactor.
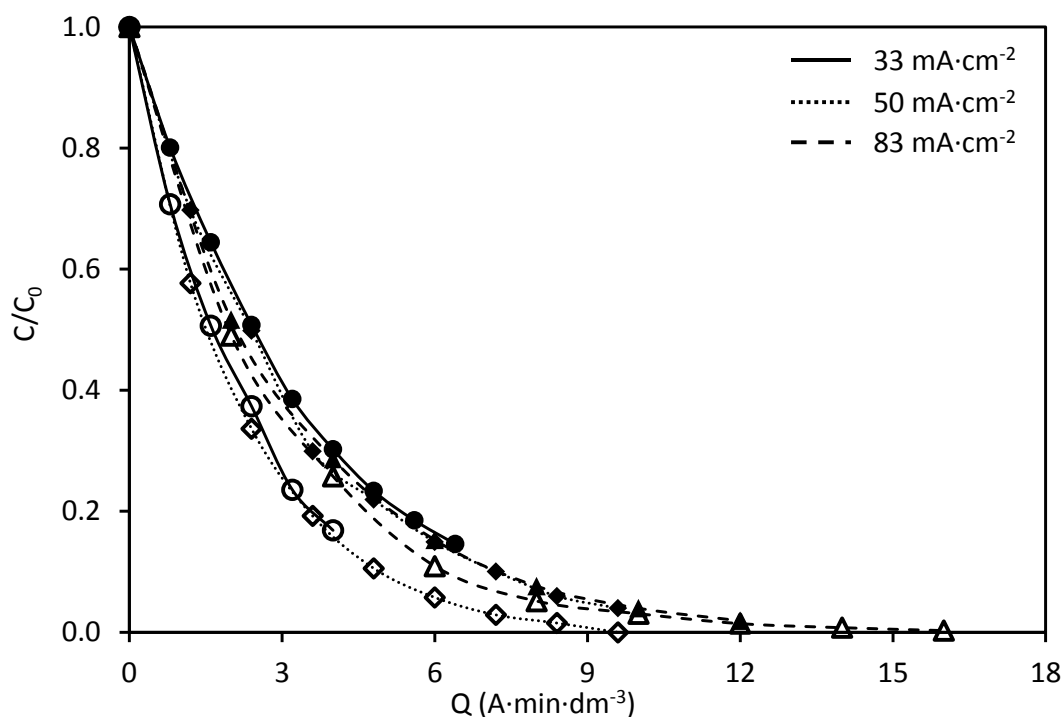

Figure 3 b). Effect of i on the decay of the relative concentration of NOR as a function of the applied charge per unit volume of electrolyzed solution for the ceramic electrode. Solid points represent the reactor without membrane and empty points the membrane reactor.

The decay of the relative NOR concentration with the electrolysis time follows an exponential trend for both types of electrodes and reactors, according with a pseudo-first-order kinetics typical of a mass transfer controlled process, which is predicted by Equation (4). This behavior is indicative of the formation of a steady concentration of reactive ·OH at each current density, which is much greater than that of NOR reaching the electrode surface [34,36,39]:

$$ln\frac{C_0}{C} = -k_{app}\, t$$

(4)

The fitting of the NOR concentration values to the previous equation gives good linear correlations as shown in the inset of Figures 2 a) and 3 a). From these results, the apparent kinetic constant values (k_{app}) are calculated, and are presented in Figure 4. As observed, higher values of k_{app} are always obtained in the divided reactor regardless of the anode under study since the velocity of the NOR degradation is higher in the presence of the cation-exchange membrane, as mentioned previously. However, the fact that k_{app} is not directly proportional to i, suggests that a smaller proportion of the generated ·OH becomes inefficient to react with organics as current density rises. This fact affects mineralization current efficiency (MCE) as will be better clarified below.
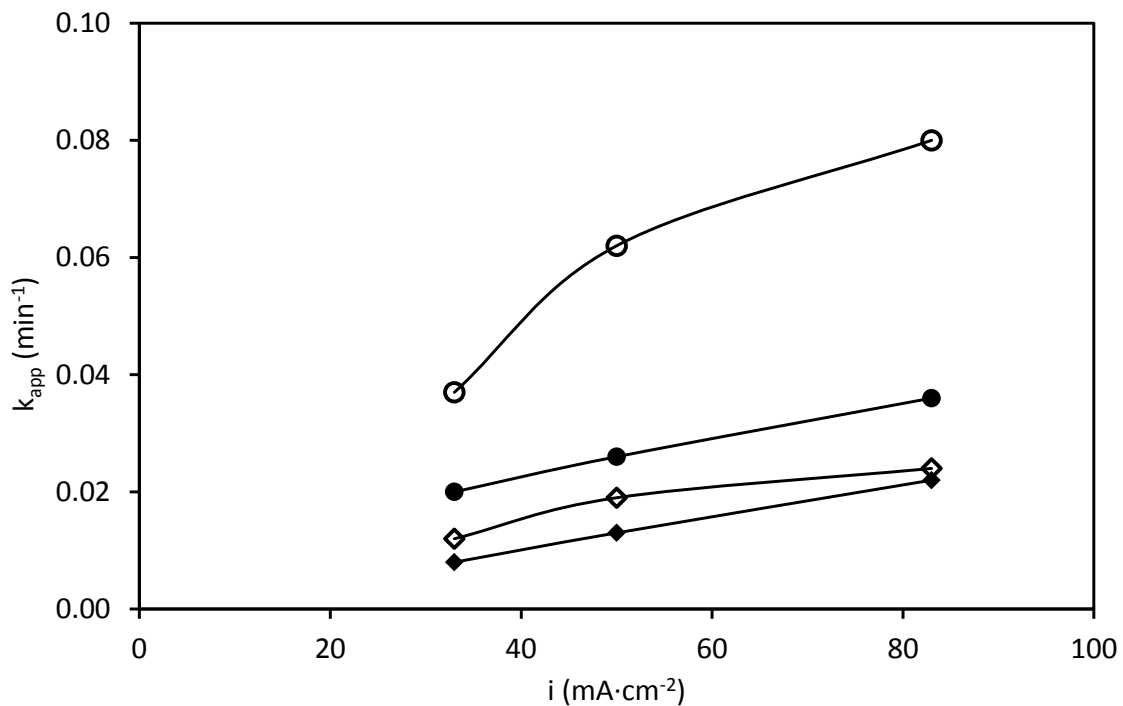

Figure 4. Effect of i on the apparent kinetic constant: BDD electrode in the undivided reactor (●), BDD electrode in the divided reactor (o), ceramic electrode in the undivided reactor (♦), ceramic electrode in the divided reactor (◊).

According to these data, it is inferred that the BDD electrode is more active than the ceramic one. This activity difference can be partially explained by the difference in the hydroxyl radical concentrations at the different electrode surfaces (S). It has been well established that anodic oxidation of organic pollutants in the potential region of O_2 evolution on the BDD and Sb-SnO$_2$ electrodes involve generation of adsorbed hydroxyl radicals, S($\cdot$OH) [40]:

$$S + H_2O \rightarrow S(\cdot OH) + H^+ + e^- \tag{5}$$

S($\cdot$OH) can then either be further oxidized to generate O_2 gas, or react with pollutants (R) to produce CO_2, H_2O, etc:

$$S(\cdot OH) \rightarrow S + 0.5O_2 + H^+ + e^- \tag{6}$$
$$R + S(\cdot OH) \rightarrow S + CO_2 + H_2O + \dots \tag{7}$$

Usually, reaction (5) is easy, and thus not a rate-determining step. The activity of an electrode is highly dependent on the rate of reaction (6). Since the BDD electrode has much higher overpotential for O_2 evolution than the Sb-SnO$_2$ ceramic electrode, the rate of reaction (6) on the BDD electrode should be much lower than that of the ceramic one. This leads to a more significant accumulation of the hydroxyl radicals on the BDD electrode surface, and therefore it can oxidize pollutants more effectively under the same conditions. Moreover, diamond is well known to have weak adsorption properties due to its inert surface. Therefore, the hydroxyl radicals produced on the BDD electrode are very weakly adsorbed and accordingly are very reactive in pollutant oxidation. In contrast, the hydroxyl radicals produced on the ceramic electrode are expected to be more strongly adsorbed and are less reactive towards pollutant oxidation [38].

The previous differences observed between both materials are also evident in the evolution of the UV-visible spectra as a function of the electrolysis time as shown in Figure 5, where two peaks in the ultraviolet region are mainly observed. One peak at 275 nm, which is associated with the aromatic ring absorption, and another peak at 330 nm caused by the quinolones nitrogen atom with n→π* (HOMO–LUMO) electronic transition [32]. After degradation, the absorption intensity decreased at 330 nm, indicating the degradation of the quinolone, while the decreased absorbance at 275 nm suggests the opening of the aromatic ring [41]. Comparing the different reactors, it is inferred that the height of both peaks decreases faster in the divided reactor as the velocity of the NOR degradation is higher.

As observed, in the case of the BDD electrode, Figures 5 a) and b), both peaks reduce their height as the electrolysis proceeds, reaching their complete disappearance at 90

minutes in the divided reactor, and 180 minutes in the undivided one. At the same time, a new absorption band appears for a wavelength range from 200 to 220 nm which is probably due to the presence of oxidation by-products in the form of short chain carboxylic acids [19]. According to the work of García-Segura et al. [42], the high concentration of these species, which are formed as a previous step to the CO_2 generation, is a further indication of the high oxidation power of the BDD anode.

In the case of the ceramic electrode, Figures 5 c) and d), the decrease of the absorbance peak at 275 nm is less significant, indicating that the aromatic rings of the molecule are less affected by the electrolysis process. After 4 h of treatment, this peak still is evident; this indicates the persistence of the aromatic rings. This fact also explains why the absorption range between 200 to 220 nm remains almost invariable with time, since the formation of the carboxylic acids mainly takes place after the oxidative ring opening reactions.
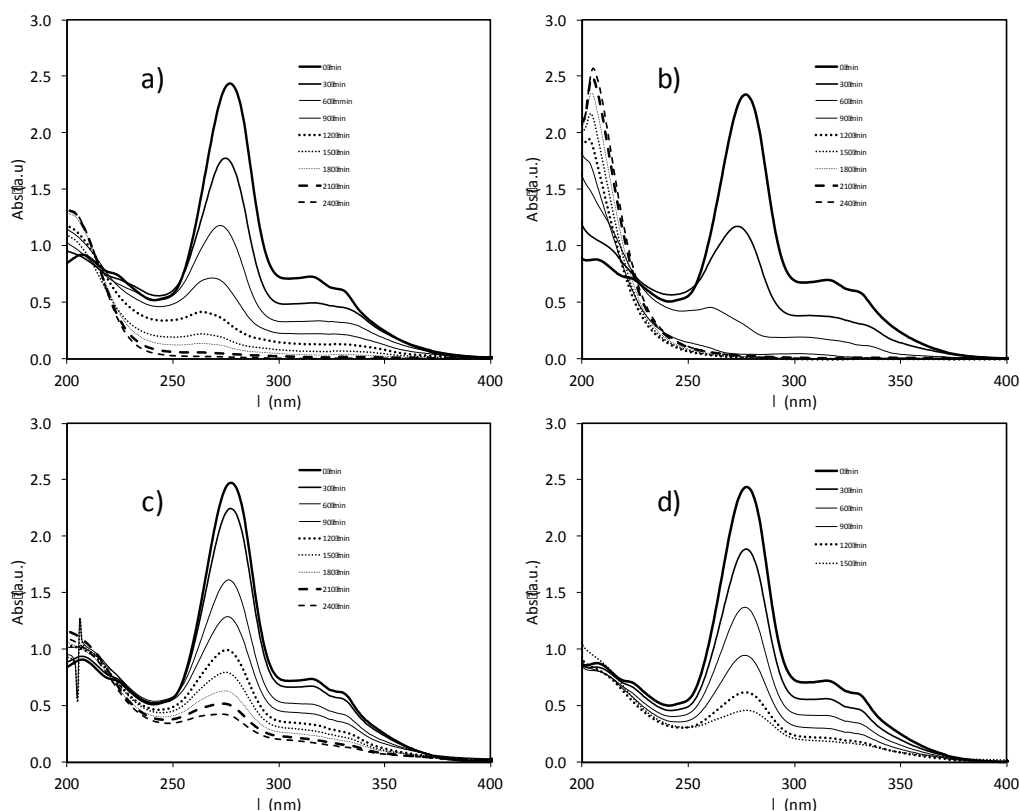

Figure 5. Evolution of the UV-visible spectra with the electrolysis time for a current density of 33 mA·cm^{-2} in the following conditions: a) BDD electrode in undivided reactor, b) BDD electrode in divided reactor, c) ceramic electrode in undivided reactor, d) ceramic electrode in divided reactor.

The degree of NOR mineralization was monitored through the total organic carbon (TOC) evolution, which represent the accumulation of all the organic compounds present in solution. The initial values of TOC measured are between 63 and 69 mg L^{-1}.

This value coincides with the theoretical value calculated for a solution composed of 100 mg·L^{-1} of NOR. The evolution of the relative TOC concentration in the divided and undivided reactors using the BDD and the ceramic electrodes is studied in Figures 6 and 7, respectively, as a function of the applied current density (i). In all the cases, the relative TOC concentration decreases with the electrolysis time as observed in Figures 6 a) and 7 a). For an electrolysis time of 30 minutes, in the case of the BDD electrode, the mineralization degree in the divided reactor was 20%, 23% and 44% for the corresponding current densities of 33, 50 and 83 mA·cm^{-2}, and 9%, 10% and 24% for the ceramic electrode in the same experimental conditions. These findings demonstrate the great oxidizing power of BDD in relation to the ceramic anode to convert NOR and all the intermediate accumulated into CO_2. In spite of this, the complete mineralization in the divided reactor is not possible for any of the applied currents under study, having a residual TOC concentration of about 5 mg L^{-1} when using the BDD. This fact suggests that carboxylic acids are still present in solution as is also confirmed by the data presented in Figure 5.

The comparative TOC abatement versus the consumed specific charge (Q) for both electrodes and reactors under study is presented in Figures 6 b) and 7 b). In both Figures, the rate of TOC removal becomes practically independent of current density in the case of the divided reactor but it decreases with i for the undivided one. The lower degree of TOC abatement at a given Q as i increases observed in the latter case can then be explained if the larger amount of hydroxyl radicals formed is destroyed more rapidly from reactions (8), (9) and (10) and hence, a lower relative proportion of this radical is able to react with organics [34] with the consequent decrease in the mineralization current efficiency, as will be discussed ahead. Nevertheless, the absolute quantity of reactive ·OH is gradually enhanced at higher i and this causes the acceleration of the degradation process with time. The greater proportion of weak oxidants (H_2O_2, HO_2 peroxodisulfate ion and ozone) formed could also contribute to mineralize some organics. In the case of the divided reactor, the results suggest the existence of a comparatively much lower enhancement of parasitic reactions with rising current density, so that the small relative proportion of reactive ·OH produced at each i remains almost unaltered leading to TOC-Q plots practically i-independent.

$$M(\cdot OH) \ \rightarrow \ M + \frac{1}{2}O_2 + H^+ + e^- \tag{8}$$

$$2M(\cdot OH) \ \rightarrow \ 2M + H_2O_2 \tag{9}$$

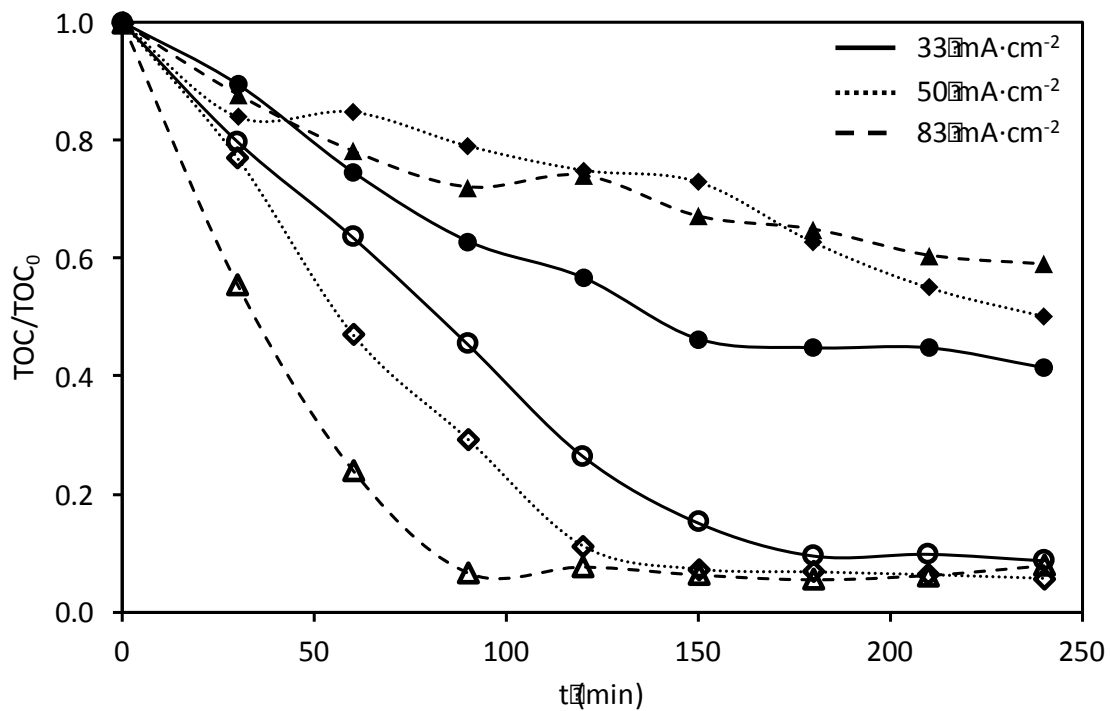$$H_2O_2 + M(\cdot OH) \ \rightarrow \ M(HO_2 \cdot) + H_2O \tag{10}$$

Figure 6 a). Effect of i on the decay of the relative TOC concentration as a function of time for the BDD electrode. Solid points represent the reactor without membrane and empty points the membrane reactor.
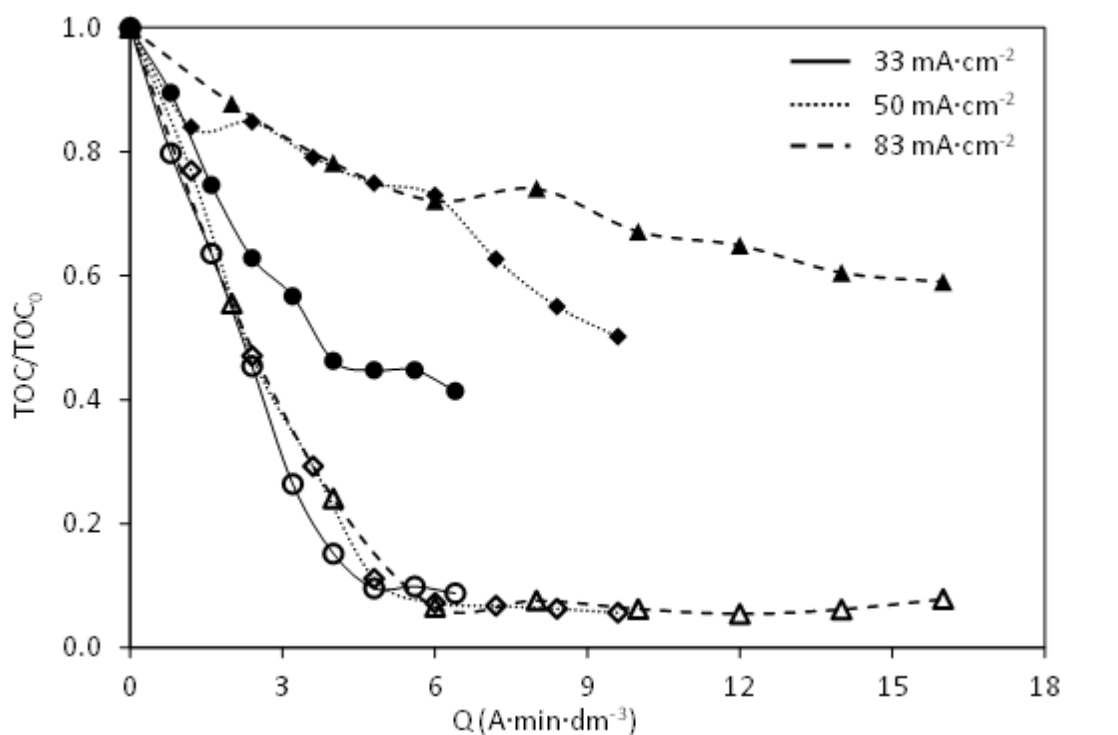

Figure 6 b). Effect of i on the decay of the relative of the relative TOC concentration as a function of the applied charge per unit volume of electrolyzed solution for the BDD electrode. Solid points represent the reactor without membrane and empty points the membrane reactor.
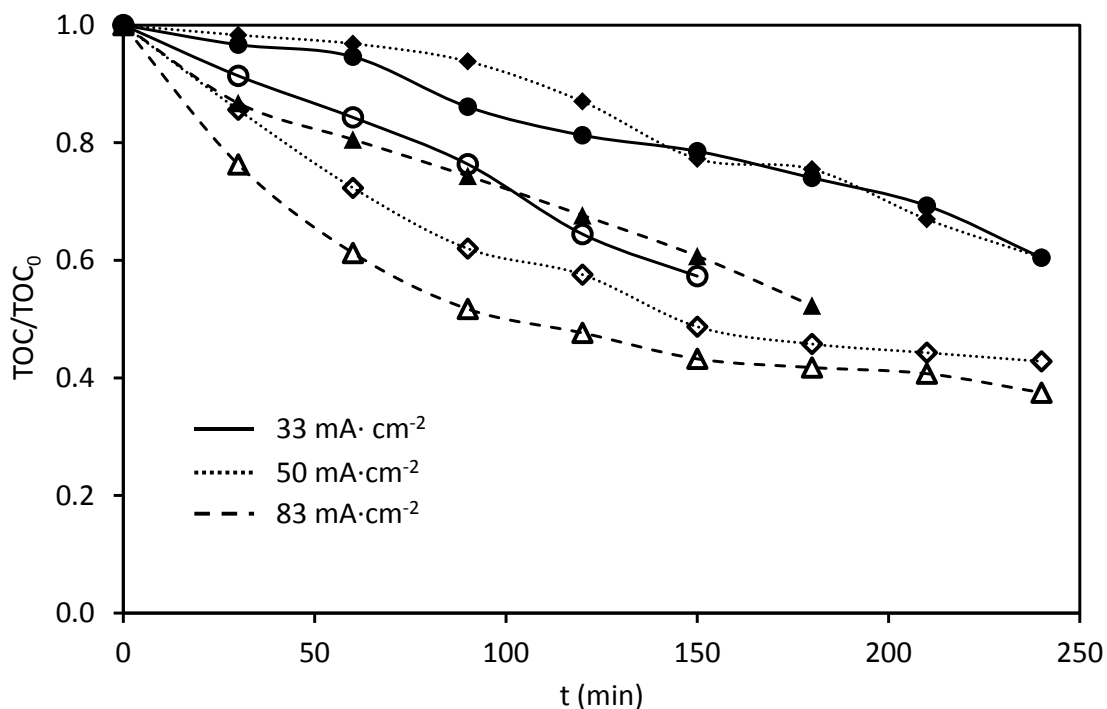
Figure 7 a). Effect of i on the decay of the relative TOC concentration as a function of time for the ceramic electrode. Solid points represent the reactor without membrane and empty points the membrane reactor.
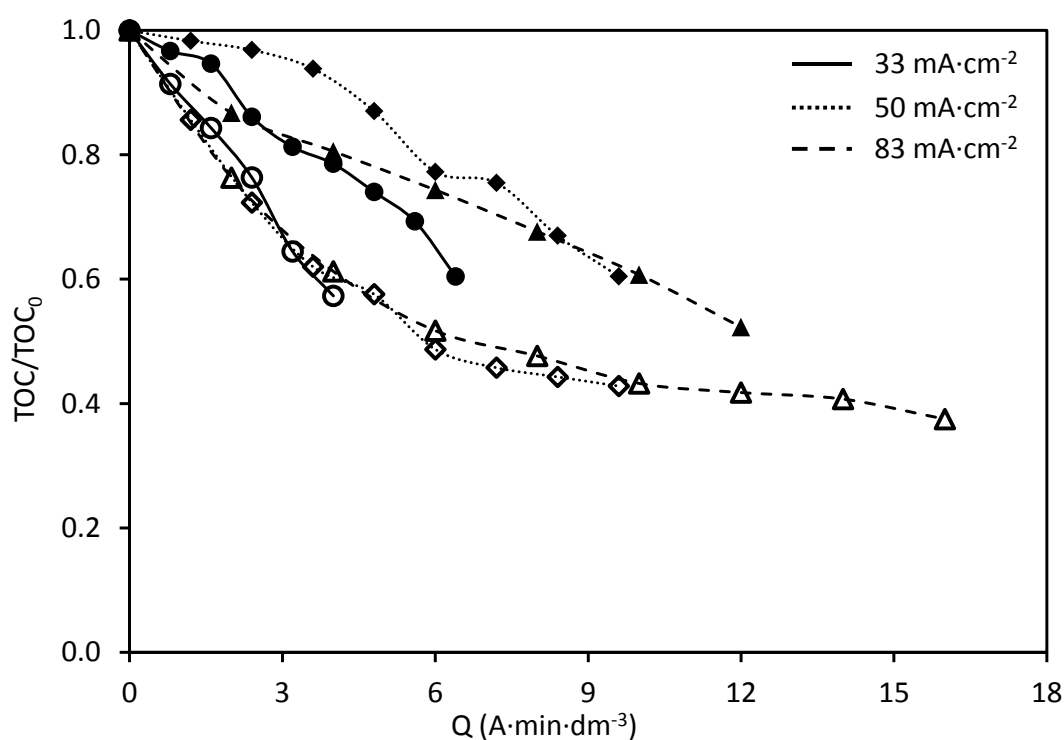

Figure 7 b). Effect of i on the decay of the relative of the relative TOC concentration as a function of the applied charge per unit volume of electrolyzed solution for the ceramic electrode. Solid points represent the reactor without membrane and empty points the membrane reactor.

16

It is inferred that the mineralization velocity is always lower than that observed for the NOR degradation under the same experimental conditions, being this difference lower as the applied current increases. The extend of the NOR mineralization (ϕ), presented in Equation (1), reflects the effect of both processes: the mineralization and the NOR degradation degree. The effect of the applied current density on ϕ for the BDD and the ceramic electrodes is presented in Figures 8 a) and b), respectively, when using the divided reactor. As observed for the BDD anode, ϕ rises with the electrolysis time and then remains practically constant for an electrolysis time between 120 minutes and 180 minutes since the NOR has been removed and the mineralization of the intermediates products of the oxidation has more weight. Besides that, the extend of the NOR mineralization (ϕ) increases with the applied current since higher values of i promotes the ·OH generation which are available to react with NOR and with all the intermediate products formed, producing its direct mineralization. In the case of the ceramic electrode, (Figure 8 b)), although the values of ϕ obtained are lower due to lowest mineralization degree obtained for this electrode, the trend of ϕ with time and applied current observed is similar to that observed for the BDD.

For both anodes under study, the presence of the membrane prevents the intermediate products produced by the NOR oxidation from being reduced on the cathode. This fact produces higher values of ϕ in the divided reactor than in the undivided one (not shown). On the other hand, comparing Figures 8 a) and b) is observed that greater values of ϕ are obtained using the BDD electrode in the divided reactor. As mentioned previously, the greater efficiency of the BDD anode is due to the very weak electrode-·OH interaction, being more ·OH available to react with NOR. The differences observed between both materials are similar to those found by other authors when comparing the BDD with other electrode materials [34,36,38,43,44].
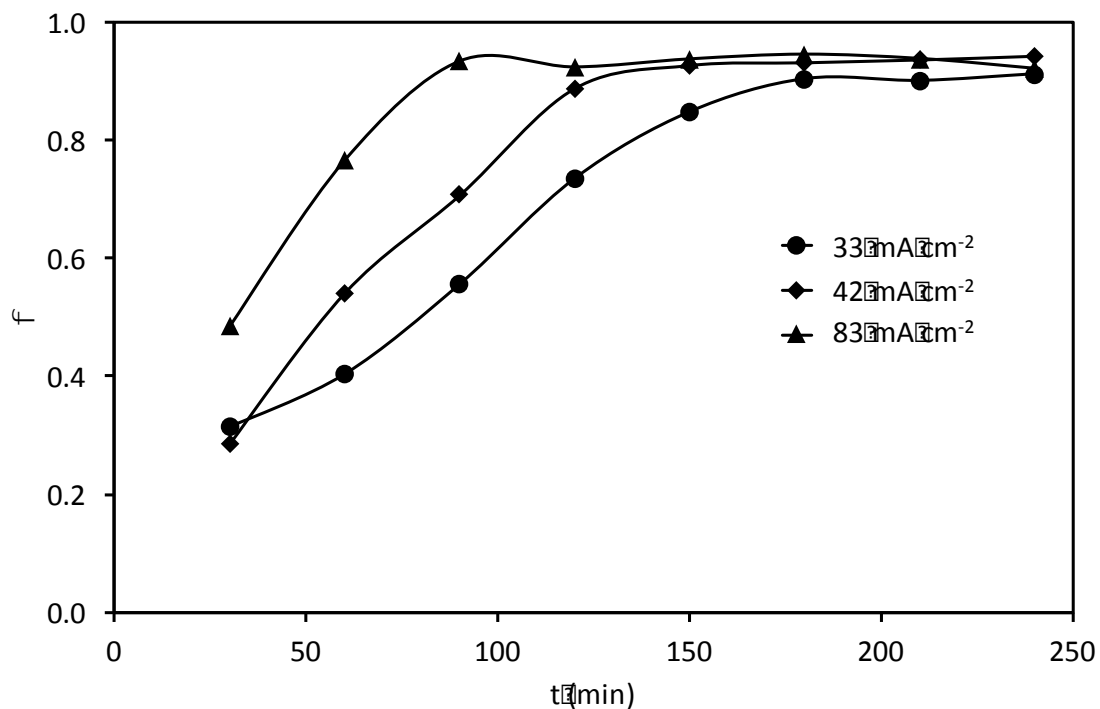
Figure 8 a). Effect of i on the extend of the NOR mineralization (φ) for the BDD electrode in the divided reactor.
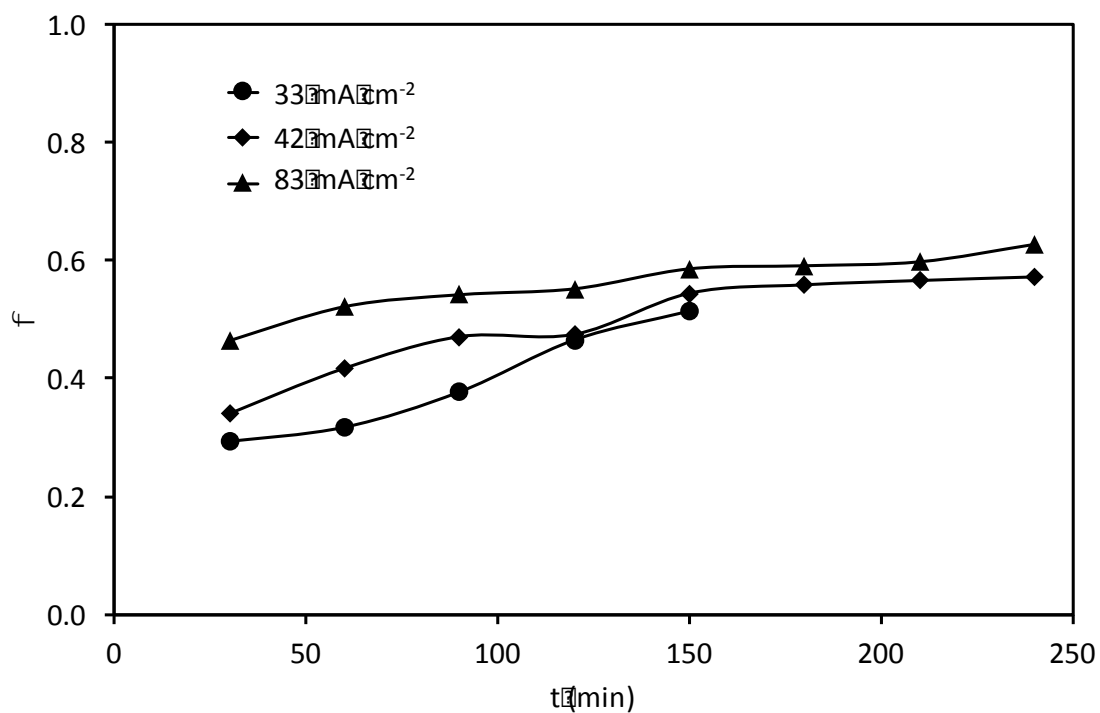

Figure 8 b). Effect of i on the extend of the NOR mineralization (φ) for the ceramic electrode in the divided reactor.

Figures 9 a) and b) show the effect of the applied current density on the mineralization current efficiency (MCE), calculated using Equation (2), for the BDD and the ceramic electrodes, respectively. For both electrodes and reactors, the higher values of MCE are obtained at the beginning of the electrolysis process which indicates a rapid conversion of the intermediate products into CO_2 during the first stages of the process, due to the $\cdot OH$ radicals generated. MCE decreases with time and low values are obtained at the end of the experiments due to the small TOC concentration. The diminution of MCE with time could be related to the formation of intermediate products more difficult to be oxidized by the $\cdot OH$ than the initial compound, such as carboxylic acids, or with the mass transfer limitations [34,35].

In the case of the BDD electrode, the average mineralization current efficiency values in the undivided reactor were 7.8%, 3.9% and 2.4% for the corresponding current densities of 33, 50 and 83 mA·cm^{-2}, and 12.7%, 9.5% and 7.8% for the same current densities in the case of the divided reactor. For the ceramic electrode, these values were 3.2%, 1.8% and 3.4% in the undivided reactor, and 6.4%, 5.6% and 4.5% in the divided one. As observed, this parameter decreases with i, being this effect more acute for the BDD anode, which may be due to the lower amount of $\cdot OH$ present in solution, since this species could be rapidly transformed into O_2, reaction (8), dimerized through reaction (9), or decomposed by H_2O_2, reaction (10), as mentioned previously.

Apart from the weak oxidants H_2O_2 and $HO_2\cdot$ formed, the high oxidation power of BDD favors the production of other weak oxidizing species such as peroxodisulphate ions and ozone, reported in reactions (11) and (12) [21,34,39]. These weak oxidizing agents can also contribute to degrade the organic matter. This phenomenon could also explain the loss of proportionality of the velocity constant (k_{app}) with i observed previously in Figure 4, since there are other species capable of reacting with organics as current density rises.

$$2SO_4^{2-} \; \longrightarrow \; S_2O_8^{2-} + 2e^- \tag{11}$$
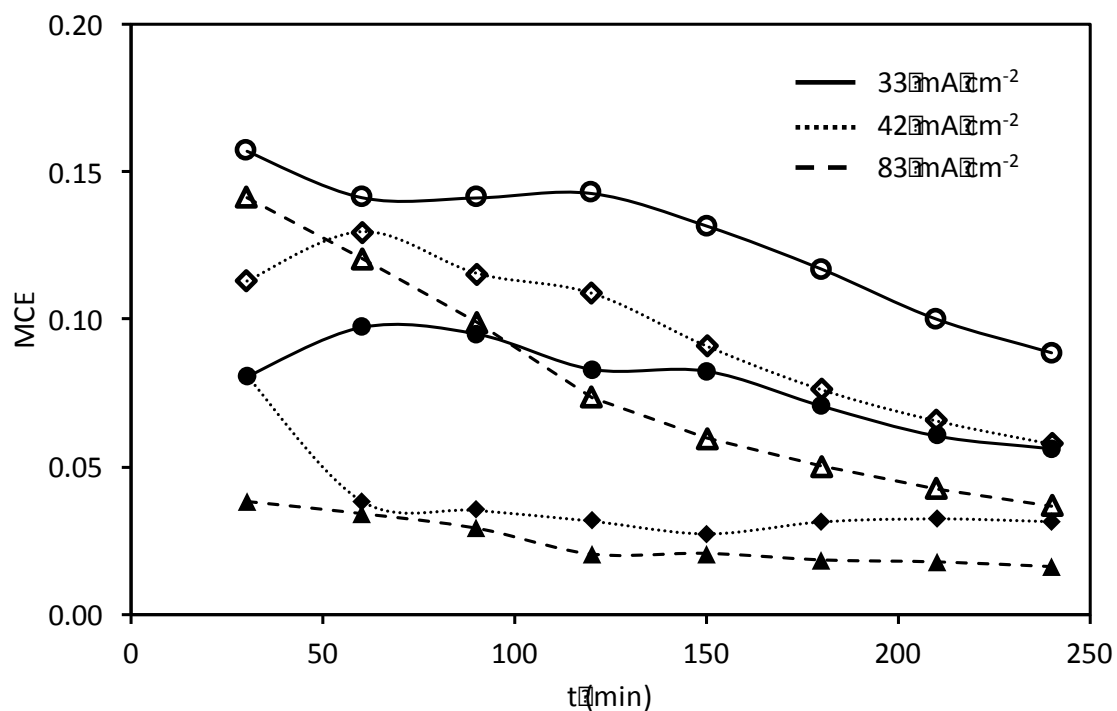$$3H_2O \; \longrightarrow \; O_3 + 6H^+ + 6e^- \tag{12}$$

Figure 9 a). Effect of i on the mineralization current efficiency (MCE) as a function of time for the BDD electrode. Solid points represent the reactor without membrane and empty points the membrane reactor.
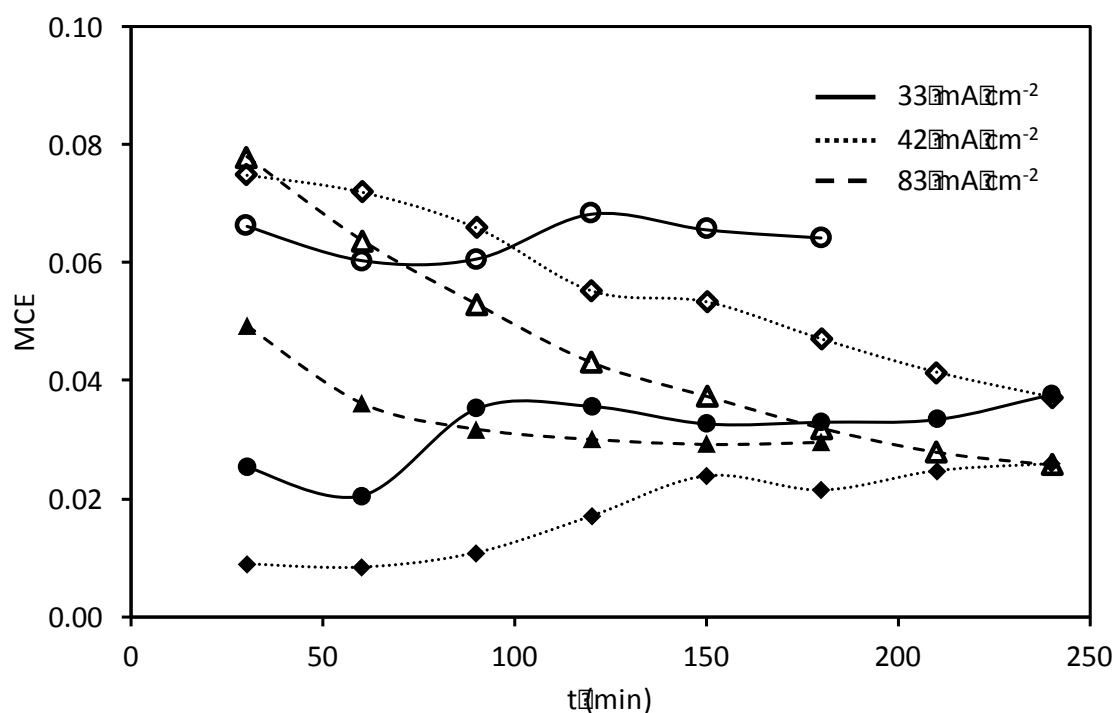

Figure 9 b). Effect of i on the mineralization current efficiency (MCE) as a function of time for the ceramic electrode. Solid points represent the reactor without membrane and empty points the membrane reactor.

Comparing both Figures 9 a) and b), it is inferred the beneficial effect of the membrane, since for the same applied current MCE is higher in the divided reactor for both electrodes. Although these values are low, they are typical of electrochemical oxidation processes of organic compounds with low TOC content [45].

The main drawback of the membrane is the associated increase of the ohmic drop that produces an increase of the energy consumption, however, its presence reduces the parasite currents, since it avoids the formation of redox couples involving species that after oxidization at the anode could be reduced at the cathode. This positive effect is higher as the current increases. Similar results are obtained by other authors [3,46].

4. **Conclusion**

Two different types of electrodes have been studied for the electrochemical oxidation of Norfloxacin (NOR) in an electrochemical reactor in the presence and absence of an ion exchange membrane. The electrochemistry of the oxidation process strongly depends on the anode type: the Sb-doped SnO_2 ceramic anode has lower oxidation power with lower values of TOC removal, while BDD acting as a typical anode with high oxidation power mineralizes the organic content to CO_2. In spite of this, the results obtained in this work demonstrate that the electrochemical oxidation of NOR is an attractive method using both types of anodes, especially in an electromembrane reactor.

The use of the membrane to separate the anodic and cathodic compartments is highly favorable as it enhances the anodic reaction kinetics and improves the current efficiency by hampering the occurrence of parasite redox couples. This leads to an improvement of the NOR degradation, the degree of mineralization and the consequent mineralization current eficiency (MCE) that compensate the increase of the ohmic drop introduced by the membrane.

References

[1]   P. Liu, H. Zhang, Y. Feng, F. Yang, J. Zhang, Removal of trace antibiotics from wastewater: A systematic study of nanofiltration combined with ozone-based advanced oxidation processes, Chem. Eng. J. 240 (2014) 211–220. doi:10.1016/j.cej.2013.11.057.

[2]   M. Chen, W. Chu, Degradation of antibiotic norfloxacin in aqueous solution by visible-light-mediated C-TiO2 photocatalysis., J. Hazard. Mater. 219–220 (2012) 183–9. doi:10.1016/j.jhazmat.2012.03.074.

[3]   C. Carlesi Jara, D. Fino, V. Specchia, G. Saracco, P. Spinelli, Electrochemical removal of antibiotics from wastewaters, Appl. Catal. B Environ. 70 (2007) 479–487. doi:10.1016/j.apcatb.2005.11.035.

[4]   M. Al Aukidy, P. Verlicchi, A. Jelic, M. Petrovic, D. Barcelò, Monitoring release of pharmaceutical compounds: Occurrence and environmental risk assessment of two WWTP effluents and their receiving bodies in the Po Valley, Italy, Sci. Total Environ. 438 (2012) 15–25. doi:10.1016/J.SCITOTENV.2012.08.061.

[5]   Q. Tuc Dinh, F. Alliot, E. Moreau-Guigon, J. Eurin, M. Chevreuil, P. Labadie, Q.T. Dinh, F. Alliot, E. Moreau-Guigon, J. Eurin, M. Chevreuil, P. Labadie, Measurement of trace levels of antibiotics in river water using on-line enrichment and triple-quadrupole LC-MS/MS., Talanta. 85 (2011) 1238–45. doi:10.1016/j.talanta.2011.05.013.

[6]   C. Wang, H. Shi, C.D. Adams, S. Gamagedara, I. Stayton, T. Timmons, Y. Ma, Investigation of pharmaceuticals in Missouri natural and drinking water using high performance liquid chromatography-tandem mass spectrometry, Water Res. 45 (2011) 1818–1828. doi:10.1016/J.WATRES.2010.11.043.

[7]   A.J.J. Watkinson, E.J.J. Murby, D.W.W. Kolpin, S.D.D. Costanzo, The occurrence of antibiotics in an urban watershed: from wastewater to drinking water., Sci. Total Environ. 407 (2009) 2711–23. doi:10.1016/j.scitotenv.2008.11.059.

[8]   A. Shimizu, H. Takada, T. Koike, A. Takeshita, M. Saha, Rinawati, N. Nakada, A. Murata, T. Suzuki, S. Suzuki, N.H. Chiem, B.C. Tuyen, P.H. Viet, M.A. Siringan, C. Kwan, M.P. Zakaria, A. Reungsang, Ubiquitous occurrence of sulfonamides in tropical Asian waters, Sci. Total Environ. 452–453 (2013) 108–115. doi:10.1016/J.SCITOTENV.2013.02.027.

[9]   S. Zou, W. Xu, R. Zhang, J. Tang, Y. Chen, G. Zhang, Occurrence and distribution of antibiotics in coastal water of the Bohai Bay, China: impacts of river discharge and aquaculture activities., Environ. Pollut. 159 (2011) 2913–20. doi:10.1016/j.envpol.2011.04.037.

[10]   K.-J. Huang, X. Liu, W.-Z. Xie, H.-X. Yuan, Electrochemical behavior and voltammetric determination of norfloxacin at glassy carbon electrode modified with multi walled carbon nanotubes/Nafion., Colloids Surf. B. Biointerfaces. 64 (2008) 269–74. doi:10.1016/j.colsurfb.2008.02.003.

[11]   Y. Luo, W. Guo, H.H. Ngo, L.D. Nghiem, F.I. Hai, J. Zhang, S. Liang, X.C. Wang, A review on the occurrence of micropollutants in the aquatic environment and their fate and removal during wastewater treatment, Sci. Total Environ. 473–474 (2014) 619–641. doi:10.1016/J.SCITOTENV.2013.12.065.

[12]   N.M. Vieno, H. Härkki, T. Tuhkanen, L. Kronberg, Occurrence of Pharmaceuticals in River Water and Their Elimination in a Pilot-Scale Drinking Water Treatment

Plant, Environ. Sci. Technol. 41 (2007) 5077–5084. doi:10.1021/es062720x.

[13] J.L. Acero, F.J. Benitez, A.I. Leal, F.J. Real, F. Teva, Membrane filtration technologies applied to municipal secondary effluents for potential reuse, J. Hazard. Mater. 177 (2010) 390–398. doi:10.1016/J.JHAZMAT.2009.12.045.

[14] J.L. Acero, F.J. Benitez, F. Teva, A.I. Leal, Retention of emerging micropollutants from UP water and a municipal secondary effluent by ultrafiltration and nanofiltration, Chem. Eng. J. 163 (2010) 264–272. doi:10.1016/J.CEJ.2010.07.060.

[15] V.R.A. Ferreira, C.L. Amorim, S.M. Cravo, M.E. Tiritan, P.M.L. Castro, C.M.M. Afonso, Fluoroquinolones biosorption onto microbial biomass: activated sludge and aerobic granular sludge, Int. Biodeterior. Biodegradation. 110 (2016) 53–60. doi:10.1016/J.IBIOD.2016.02.014.

[16] B.O. Pan, B. Xing, Critical Review Adsorption Mechanisms of Organic Chemicals on Carbon Nanotubes, (2008) 9005–9013.

[17] X. Wu, M. Huang, T. Zhou, J. Mao, Recognizing removal of norfloxacin by novel magnetic molecular imprinted chitosan/γ-Fe2O3 composites: Selective adsorption mechanisms, practical application and regeneration, Sep. Purif. Technol. 165 (2016) 92–100. doi:10.1016/J.SEPPUR.2016.03.041.

[18] E. Brillas, I. Sirés, M.A. Oturan, Electro-Fenton Process and Related Electrochemical Technologies Based on Fenton 's Reaction Chemistry, Chem. Rev. 109 (2009) 6570–6631. doi:10.1021/cr900136g.

[19] D.A.C. Coledam, J.M. Aquino, B.F. Silva, A.J. Silva, R.C. Rocha-Filho, Electrochemical mineralization of norfloxacin using distinct boron-doped diamond anodes in a filter-press reactor, with investigations of toxicity and oxidation by-products, Electrochim. Acta. 213 (2016) 856–864. doi:10.1016/j.electacta.2016.08.003.

[20] S.D. Jojoa-Sierra, J. Silva-Agredo, E. Herrera-Calderon, R.A. Torres-Palma, Elimination of the antibiotic norfloxacin in municipal wastewater, urine and seawater by electrochemical oxidation on IrO 2 anodes, Sci. Total Environ. 575 (2017) 1228–1238. doi:10.1016/j.scitotenv.2016.09.201.

[21] M. Panizza, G. Cerisola, Direct And Mediated Anodic Oxidation of Organic Pollutants, Chem. Rev. 109 (2009) 6541–6569. doi:10.1021/cr9001319.

[22] E. Brillas, C.A. Martínez-Huitle, Decontamination of wastewaters containing synthetic organic dyes by electrochemical methods. An updated review, Appl. Catal. B Environ. 166–167 (2015) 603–643. doi:10.1016/j.apcatb.2014.11.016.

[23] M. Panizza, G. Cerisola, Application of diamond electrodes to electrochemical processes, Electrochim. Acta. 51 (2005) 191–199. doi:10.1016/j.electacta.2005.04.023.

[24] Y. Wang, C. Shen, M. Zhang, B.-T. Zhang, Y.-G. Yu, The electrochemical degradation of ciprofloxacin using a SnO 2 -Sb/Ti anode: Influencing factors, reaction pathways and energy demand, (2016). doi:10.1016/j.cej.2016.03.093.

[25] L. Lipp, D. Pletcher, The preparation and characterization of tin dioxide coated titanium electrodes, Hecrrochimico Acta. 42 (1997) 1091–1099.

[26] S.-Y. Park, S.-I. Mho, E.O. Chi, Y.U. Kwon, H.L. Park, Characteristics of Pt thin films on the conducting ceramics TiO and Ebonex (Ti4O7) as electrode materials, Thin Solid Films. 258 (1995) 5–9. doi:10.1016/0040-6090(94)09477-2.

[27] S. Zuca, M. Terzi, M. Zaharescu, K. Matiasovsky, Contribution to the study of

SnO2-based ceramics, J. Mater. Sci. 26 (1991) 1673–1676. doi:10.1007/BF00544681.

[28] D. Bejan, J.D. Malcolm, L. Morrison, N.J. Bunce, Mechanistic investigation of the conductive ceramic Ebonex® as an anode material, Electrochim. Acta. 54 (2009) 5548–5556. doi:10.1016/j.electacta.2009.04.057.

[29] G. Chen, E. a. Betterton, R.G. Arnold, Electrolytic oxidation of trichloroethylene using a ceramic anode, J. Appl. Electrochem. 29 (1999) 961–970. doi:10.1023/A:1003541706456.

[30] A.M. Zaky, B.P. Chaplin, Porous substoichiometric TiO2 anodes as reactive electrochemical membranes for water treatment, Environ. Sci. Technol. 47 (2013) 6554–6563. doi:10.1021/es401287e.

[31] J. Mora-Gómez, M. García-Gabaldón, E. Ortega, M.-J. Sánchez-Rivera, S. Mestre, V. Pérez-Herranz, Evaluation of new ceramic electrodes based on Sb-doped SnO2 for the removal of emerging compounds present in wastewater, Ceram. Int. 44 (2018) 2216–2222. doi:10.1016/J.CERAMINT.2017.10.178.

[32] U. Neugebauer, A. Szeghalmi, M. Schmitt, W. Kiefer, J. Popp, U. Holzgrabe, Vibrational spectroscopic characterization of fluoroquinolones, Spectrochim. Acta Part A Mol. Biomol. Spectrosc. 61 (2005) 1505–1517. doi:10.1016/J.SAA.2004.11.014.

[33] D.W. Miwa, G.R.P. Malpass, S.A.S. Machado, A.J. Motheo, Electrochemical degradation of carbaryl on oxide electrodes, Water Res. 40 (2006) 3281–3289. doi:10.1016/J.WATRES.2006.06.033.

[34] M. Hamza, R. Abdelhedi, E. Brillas, I. Sirés, Comparative electrochemical degradation of the triphenylmethane dye Methyl Violet with boron-doped diamond and Pt anodes, J. Electroanal. Chem. 627 (2009) 41–50. doi:10.1016/j.jelechem.2008.12.017.

[35] E. Guinea, J.A. Garrido, R.M. Rodríguez, P.-L. Cabot, C. Arias, F. Centellas, E. Brillas, Degradation of the fluoroquinolone enrofloxacin by electrochemical advanced oxidation processes based on hydrogen peroxide electrogeneration, Electrochim. Acta. 55 (2010) 2101–2115. doi:10.1016/j.electacta.2009.11.040.

[36] A. Özcan, A. Atılır Özcan, Y. Demirci, Evaluation of mineralization kinetics and pathway of norfloxacin removal from water by electro-Fenton treatment, Chem. Eng. J. 304 (2016) 518–526. doi:10.1016/j.cej.2016.06.105.

[37] M. Panizza, A. Kapalka, C. Comninellis, Oxidation of organic pollutants on BDD anodes using modulated current electrolysis, Electrochim. Acta. 53 (2008) 2289–2295. doi:10.1016/j.electacta.2007.09.044.

[38] X. Chen, F. Gao, G. Chen, Comparison of Ti/BDD and Ti/SnO2-Sb2O5 electrodes for pollutant oxidation, J. Appl. Electrochem. 35 (2005) 185–191. doi:10.1007/s10800-004-6068-0.

[39] C. Flox, J.A. Garrido, R.M. Rodríguez, F. Centellas, P.-L. Cabot, C. Arias, E. Brillas, Degradation of 4,6-dinitro-o-cresol from water by anodic oxidation with a boron-doped diamond electrode, Electrochim. Acta. 50 (2005) 3685–3692. doi:10.1016/j.electacta.2005.01.015.

[40] B. Correa-Lozano, C. Comninellis, A. de Battisti, Service life of Ti/SnO2–Sb2O5 anodes, J. Appl. Electrochem. 27 (1997) 970–974. doi:10.1023/A:1018414005000.

[41] L. Chen, H. Zhou, Q. Deng, Photolysis of nonylphenol ethoxylates: The

determination of the degradation kinetics and the intermediate products, Chemosphere. 68 (2007) 354–359. doi:10.1016/J.CHEMOSPHERE.2006.12.055.

[42]   S. Garcia-Segura, E. Brillas, Mineralization of the recalcitrant oxalic and oxamic acids by electrochemical advanced oxidation processes using a boron-doped diamond anode, Water Res. 45 (2011) 2975–2984. doi:10.1016/J.WATRES.2011.03.017.

[43]   A.J.C. da Silva, E.V. dos Santos, C.C. de Oliveira Morais, C.A. Martínez-Huitle, S.S.L. Castro, Electrochemical treatment of fresh, brine and saline produced water generated by petrochemical industry using Ti/IrO2–Ta2O5 and BDD in flow reactor, Chem. Eng. J. 233 (2013) 47–55. doi:10.1016/j.cej.2013.08.023.

[44]   G.F. Pereira, B.F. Silva, R. V. Oliveira, D.A.C. Coledam, J.M. Aquino, R.C. Rocha-Filho, N. Bocchi, S.R. Biaggio, Comparative electrochemical degradation of the herbicide tebuthiuron using a flow cell with a boron-doped diamond anode and identifying degradation intermediates, Electrochim. Acta. (2017). doi:10.1016/j.electacta.2017.07.054.

[45]   C.A. Martínez-Huitle, M.A. Rodrigo, I. Sirés, O. Scialdone, Single and Coupled Electrochemical Processes and Reactors for the Abatement of Organic Water Pollutants: A Critical Review, Chem. Rev. 115 (2015) 13362–13407. doi:10.1021/acs.chemrev.5b00361.

[46]   A. El-Ghenymy, F. Centellas, J.A. Garrido, R.M. Rodríguez, I. Sirés, P.L. Cabot, E. Brillas, Decolorization and mineralization of Orange G azo dye solutions by anodic oxidation with a boron-doped diamond anode in divided and undivided tank reactors, Electrochim. Acta. 130 (2014) 568–576. doi:10.1016/j.electacta.2014.03.066.